Supporting Information

2D Hydrogenated Boride as Reductant and Stabilizer for in-situ Synthesis of Ultrafine and Surfactant-Free Carbon Supported Noble Metal Electrocatalysts with Enhanced Activity and Stability

Saisai Gao,[a] Yang Zhang,[a] Jinglei Bi,[a] Bin Wang,[a]* Chao Li,[b] Jiamei Liu,[b] Chuncai Kong,[a] Sen Yang[a] and Shengchun Yang[ac]*

a. MOE Key Laboratory for Non-equilibrium Synthesis and Modulation of Condensed Matter, State Key Laboratory for Mechanical Behavior of Materials, Key Laboratory of Shaanxi for Advanced Materials and Mesoscopic Physics, School of Physics, Xi'an Jiaotong University, Xi'an 710049, P. R. China. E-mail: *bin_wang@xjtu.edu.cn* and *ysch1209@mail.xjtu.edu.cn*

b. Instrumental Analysis Center of Xi'an Jiaotong University，Xi'an Jiaotong University, Xi'an 710049, P. R. China.

c. Cooperation Agreement on co-construction of Shenshupan/Jinbaolige Mining, Xi'an Jiaotong University Joint R&D Center, Xi'an 710049, P. R. China.

Experimental section:

Materials: MgB_2 (99.9%, 200 mesh) and ion-exchange resin (Amberlite IR120, H^+ form) were obtained from Macklin Reagent. Methanol (AR, 99.9%) was purchased from Sinopharm Group Chemical Reagent. Graphitized carbon black (Vulcan XC-72, Cabot) was supplied by Cabot Carbon Ltd. Nafion solution (5 wt.%) was purchased from Aldrich. K_2PtCl_4, K_2PdCl_4 and $KAuCl_4$ were purchased from Kunming Institute of Precious Metals. Commercial Pt/C (20 wt.%) and commercial Pd/C (10 wt.%) were purchased from Alfa Aesar chemical Co Ltd. All the chemicals were analytical grade and used as received. Deionized water (18.25 MΩ/cm) was used throughout the experiments.

Preparation of ultrafine noble metal nanoparticles on B-C supports:

Firstly, the HB was prepared by the ion exchange method.[1] Typically, 60 mg MgB_2 powder was added to 200 mL of methanol, followed by ultrasonication for 30 min in an ice bath. The prepared suspension was then added to a methanol suspension (100 mL) containing the ion-exchange resin (30 mL) under nitrogen at room temperature. After stirring at 250 rpm for 3 d under nitrogen, the supernatant was evaporated on an oil bath at 343 K under nitrogen. The HB methanol dispersion was obtained until the volume of the supernatant evaporates to about 10 ml.

The Pt/B-C (21.2 wt.%, determined by ICP-MS) catalyst was prepared by a facile magnetic stirring method without any surfactants, capping agents or reductants. A typical procedure was performed as follows: 24 mg graphitized carbon black (Vulcan XC-72, Cabot) was uniformly dispersed in 10 ml methanol by ultrasonic dispersion. Then, 10 ml HB methanol dispersion was added into the above carbon black dispersion, and ultrasonic treatment for 2 hours to obtain the carbon black loaded HB (HB-C) composite support dispersion. Lastly, 615 μl K_2PtCl_4 aqueous solution (50 mM) was

added into the HB-C dispersion dropwise under magnetic stirring. After magnetic stirring at room temperature for 12 hours, the precipitates were harvested by centrifugation and washed thoroughly with and ethanol deionized water.

The Pt/B-C catalyst was obtained by drying the black solid product at 50 °C in the vacuum drying oven overnight. The Pt/B-C (35.5 and 52.9 wt.% , determined by ICP-MS) was prepared by the same process in the condition that the dosage of the K_2PtCl_4 aqueous solution was adjusted.

The Pt/B was prepared by the same process without the addition of the carbon black.

The BC was prepared by the same process in the condition that the K_2PtCl_4 aqueous solution was replaced by the same volume of deionized water.

The Pd/B-C and Au/B-C catalysts with different loading amounts (20 and 40 wt. %, determined by the materials feed ratio) were also prepared according to the above method using different doses K_2PdCl_4 and $KAuCl_4$ aqueous solution as the metal precursors.

Characterization:

TEM, HRTEM, HAADF-STEM and elemental mapping analysis were taken on a JEOL JEM-F200 instrument equipped with energy-dispersive X-ray spectroscopy (EDX) at an accelerating voltage of 300 kV. EELS analysis was performed on an aberration-corrected FEI Titan 80-300 ETEM G2 at 300 kV. XRD patterns were acquired on a LabX XRD-6100 X-ray diffractometer by using Cu Kα radiation source (λ= 1.5406 A), operating at 40 kV and 30 mA. XPS was carried out on a Thermo Fisher Scientific ESCALAB Xi+ spectrometer with an Al Kα radiator. FTIR spectra were obtained on Thermo Fisher Scientific Nicolet iS50 FTIR Spectrometer. The Pt mass loadings in the as-prepared catalysts were determined by a NexION 350D ICP-MS inductively coupled plasma atomic emission spectroscopy.

Electrochemical measurements:

All the electrochemical measurements were conducted on an electrochemical workstation (CHI 760) in a typical three-electrode system at room temperature. To prepare the catalyst loaded electrode, the catalyst was dispersed in the mixture of water, isopropanol and 5 wt.% Nafion (v/v/v = 4:1:0.025) solvent, ultrasonicated for 30 min to form a homogeneous catalysts ink. Then the catalyst ink was loaded onto rotating disk electrode (RDE, for ORR and HER) or glassy carbon electrode (GCE, for MOR) with a geometric area of 0.196 cm^{-2} to achieve the loading amount of Pt at 2 μg for commercial Pt/C and Pt/B-C catalysts, respectively(based on ICP-MS). Prior to the surface modification, the electrodes were respectively polished with 0.5 μm and 50 nm alumina slurries to obtain a mirror-like surface, and finally rinsed with Milli-Q water under an ultrasonic bath for 1 min.

For the MOR measurements of commercial Pt/C and as-prepared Pt/B-C, the 0.5 M H_2SO_4 and 0.5 M H_2SO_4+0.5 M CH_3OH electrolyte solution was saturated with N_2 by bubbling N_2 prior to each measurement respectively for CVs and catalytic performance of MOR. The GCE loaded with catalyst was used as working electrode, a graphite rod as counter electrode, and a mercury/mercurous sulfate electrode (MSE) as reference electrode in 0.5 M H_2SO_4. After the CV curves became stable with a scan rate of 150 mV s^{-1}, a CV curve was obtained in the voltage range between 0 and 1.2 V (vs RHE) with a scan rate of 50 mV s^{-1}. The electrochemical active surface area (ECSA) can be calculated by integrating the charge passing the electrode during the hydrogen adsorption/desorption process after the correction for the double layer formation. The ECSAs were calculated by equation (1):

$$ECSA = \frac{Q_H}{0.21 \times [Pt]} \quad (1)$$

where Q_H (mC) was the charge due to the hydrogen desorption in the hydrogen region (0.05-0.35 V vs RHE) of the CVs, the charge required to oxidize a hydrogen monolayer was 0.21 mC cm^{-2}, corresponding to a surface density of 1.3×10^{15} Pt atoms per cm^{-2} and [Pt] was the mass loading of Pt on the working electrode.[2]

The CVs of MOR were carried out in 0.5 M H_2SO_4+0.5 M CH_3OH electrolyte solution in the voltage range between 0 and 1.2 V (vs RHE) with a scan rate of 50 mV s^{-1}. The chronoamperometry (CA) measurement was performed in 0.5 M H_2SO_4+0.5 M CH_3OH solution at 0.85 V. And the long-term durability (continuous CA cycles) of Pt/B-C for MOR was performed by activating the aged Pt/B-C catalyst through several CV cycles in 0.5 M H_2SO_4, the 0.5 M H_2SO_4+0.5 M CH_3OH electrolyte was replaced before the next continuous CA test.

For the ORR measurements commercial Pt/C and as-prepared Pt/B-C, the 0.1 M $HClO_4$ electrolyte solution was saturated with N_2 or O_2 by bubbling N_2 or O_2 prior to each measurement respectively for CVs and catalytic performance of ORR. The RDE loaded with catalyst was used as working electrode, a graphite rod as counter electrode, and a silver/silver chloride electrode (Ag/AgCl) as reference electrode in 0.1 M $HClO_4$ with a rotation control (Pine Instruments). After the CV curves became stable with a scan rate of 150 mV s^{-1}, a CV curve was obtained in the voltage range between 0.05 and 1.2 V (vs RHE) with a scan rate of 50 mV s^{-1} in N_2-saturated 0.1 M $HClO_4$.The LSV measurements were conducted in O_2-saturated 0.1 M $HClO_4$ with a scan rate of 10 mV s^{-1}. To directly describe the intrinsic properties of the catalyst, the iR correction is used to remove the effect of ohmic resistance unless specifically stated. The ORR kinetic current (j_k) can be calculated using the following Koutecky-Levich equation (2):

$$\frac{1}{j} = \frac{1}{j_k} + \frac{1}{j_d} = \frac{1}{j_k} + \frac{1}{0.62nFAC_{O_2}D_{O_2}^{2/3}\omega^{1/2}v^{-1/6}} \quad (2)$$

where j, j_k, and j_d are the measured, the kinetic, and the diffusion-limited current density, respectively. The j_d can be determined by the number of electrons transferred (n), F is the Faraday constant, A is the geometric area of the electrode, C_{O_2} refers to the concentration of dissolved O_2 in solution, D_{O_2} represents the diffusion coefficient of O_2, v is the kinetic viscosity of the solution, and ω is the electrode rotation speed. j_k can be derived from the Koutecky-Levich plot (j^{-1} vs $\omega^{1/2}$) at various rotation speeds. The accelerated durability test (ADT) was performed between 0.6 and 1.0 V (vs RHE) at 150 mV s^{-1} for 10000 cycles in O_2-saturated 0.1 M $HClO_4$. Then the CV curves after the ADT was obtained in the voltage range between 0 and 1.2 V (vs RHE) with scan rate of 50 mV s^{-1} in N_2-saturated 0.1 M $HClO_4$. And the LSV curves after the ADT were obtained in O_2-saturated 0.1 M $HClO_4$ at 10 mV s^{-1} and an RDE rotation speed of 1600 rpm.

For the HER measurements commercial Pt/C and as-prepared Pt/B-C, the 0.5 M H_2SO_4 electrolyte solution was saturated with N_2 by bubbling N_2 prior to each measurement, and a flow of N_2 was maintained during the scanning process. The RDE loaded with catalyst was used as working electrode, a graphite rod as counter electrode, and a mercury/mercurous sulfate electrode (MSE) as reference electrode in 0.5 M H_2SO_4 with a rotation control (Pine Instruments). LSV measurements were conducted in 0.5 M H_2SO_4 with scan rate of 5 mV s^{-1}. In order to directly describe the intrinsic properties of the catalyst, the iR correction is used to remove the effect of ohmic resistance unless specifically stated. The Tafel slopes were calculated based on the Tafel equation ($\eta = b \log j + a$, where j is the current density and b is the Tafel slope). The i-t curve was conducted by the chronoamperometry measurement carried out at a constant potential to

achieve the current densities of 10 mA cm^{-2}.

For the EOR measurements of commercial Pd/C and the as-prepared Pd/B-C, the 1 M KOH and 1 M KOH+0.5 M CH_3CH_2OH electrolyte solution was saturated with N_2 by bubbling N_2 prior to each measurement respectively for CVs and catalytic performance of EOR. The GCE loaded with catalyst was used as working electrode, a graphite rod as counter electrode, and a mercury/ mercuric oxide electrode (Hg/HgO) as reference electrode in 1 M KOH. After the CV curves became stable with a scan rate of 150 mV s^{-1}, a CV curve was obtained in the voltage range between 0.05 and 1.2 V (vs RHE) with a scan rate of 50 mV s^{-1}. The CVs of EOR was carried out in 1 M KOH+0.5 M CH_3CH_2OH electrolyte solution in the voltage range between 0.05 and 1.2 V (vs RHE) with a scan rate of 50 mV s^{-1}. The chronoamperometry (CA) measurement was performed in 1 M KOH+0.5 M CH_3CH_2OH solution at 0.75 V (vs RHE).

For the ORR measurements of commercial Pt/C and Au/B-C, the 0.1 M KOH electrolyte solution was saturated with N_2 or O_2 by bubbling N_2 or O_2 prior to each measurement respectively for CVs and catalytic performance of ORR. The RDE loaded with catalyst was used as working electrode, a graphite rod as counter electrode, and a mercury/ mercuric oxide electrode (Hg/HgO) as reference electrode in 0.1 M KOH with a rotation control (Pine Instruments). After the CV curves became stable with a scan rate of 150 mV s^{-1}, a CV curve was obtained in the voltage range between 0 and 1.2 V (vs RHE) with a scan rate of 50 mV s^{-1} in N_2 or O_2-saturated 0.1 M KOH. The CV curve was also obtained in O_2-saturated 0.1 M KOH+3 M CH_3OH to evaluate the methanol tolerance for ORR of the catalysts. The LSV measurements were conducted in O_2-saturated 0.1 M KOH with a scan rate of 10 mV s^{-1}. In order to directly describe the intrinsic properties of the catalyst, the iR correction is used to remove the effect of ohmic resistance unless specifically stated. The i-t curves at 0.5 V

(vs RHE) of Au/B-C and Pt/C were also tested with an addition of methanol into 0.1 M KOH during the process to evaluate the methanol tolerance for ORR of the catalysts.

In all measurements, all the reference electrodes were calibrated with respect to reversible hydrogen electrode (RHE).

In the same way, the electrocatalytic activities of commercial Pt/C (Alfa Aesar, 20 wt %) and commercial Pd/C (Alfa Aesar, 10 wt.%) were also tested as contrasts.

Membrane electrode assembly (MEA) fabrication and single-cell test:

The catalyst activity was evaluated by PEMFC station (SMART2, WonATech). Specifically, Pt/B-C and commercial Pt/C was employed as the cathode catalysts, respectively. Commercial Pt/C (20 wt.%) was used for the anode. The catalysts were stirred and ultrasonicated in isopropanol and Nafion solution to prepare the ink. The active area of electrodes was 5 cm^2. The well-dispersed catalyst ink was sprayed onto the graphite side of the carbon paper. The Pt loading at the cathode was 0.15 mg cm^{-2} for Pt/B-C and commercial Pt/C, respectively. As for the anode, Pt/C was used with a loading of 0.15 mg cm^{-2}. The Nafion 115 membrane (DuPont) was treated with 5 wt.% H_2O_2 and 0.5 M H_2SO_4 solutions at 80 °C for 1 h each step and then washed with deionized water. Finally, the single fuel cell was assembled with two pieces of carbon paper with catalysts as gas diffusion layers on both sides of the Nafion 115 membrane by hot press treatment at 120 °C for 5 min. The H_2-O_2 PEMFC system was tested using fully humidified H_2 and O_2 at 80 °C. The cell temperature was kept at 80 °C, and the flow rate of both H_2 (29 psi) and O_2 (29 psi) gases was 300 and 600 sccm. Before the performance testing, the single cells were activated in a continuous discharge mode until a stable condition was obtained.

DFT Calculations:

All calculations were performed by using first-principles study based on the spin-polarized density functional theory (DFT) within the projector augmented wave method,[3,4] as implemented in Vienna *ab initio* simulation package (VASP).[5,6] The generalized gradient approximation (GGA) with the functional of Perdew-Burke-Ernzerhof (PBE) was employed to describe the electron exchange-correlation interactions.[7,8] The cut-off of plane-wave kinetic energy and the convergence of total energy were set to be 500 eV and 10^{-5} eV, respectively. All studied borophene and graphene layers with or without Pt adsorption were modeled in a large supercell and located in the *x*-*y* plane. Because of the application of periodic boundary conditions, a vacuum region of at least 10 Å was applied along the *z*-axis to eliminate the interactions between neighbor layers. Supercells containing 4×2 primitive cells of borophene and 3×3 primitive cells of graphene were adopted. Thence, 5×5×1 and 9×9×1 *k*-point meshes with Gamma centered grid were used to approximate the brillouin zone integrations for borophene and graphene. Structural relaxations were performed by computing the Hellmann-Feynman forces using conjugate gradient algorithm within a force convergence of 0.01 eV/Å.[9]

Figure S1. The digital photograph of HB methanol dispersion, and the distinct tyndall effect under laser irradiation.

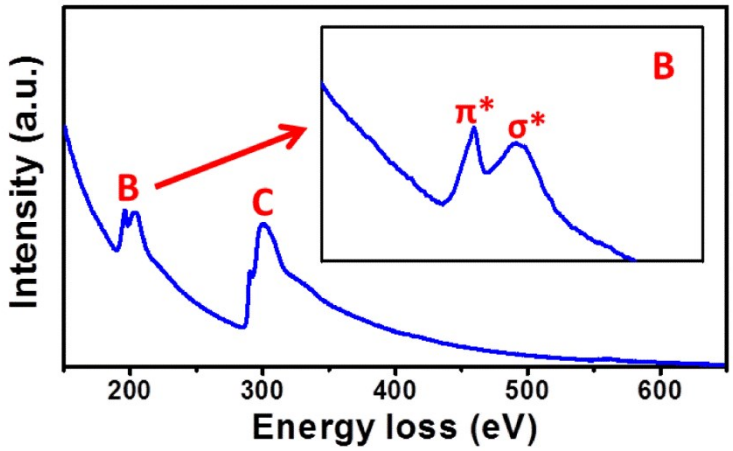

Figure S2. EELS spectrum of the HB sheets.

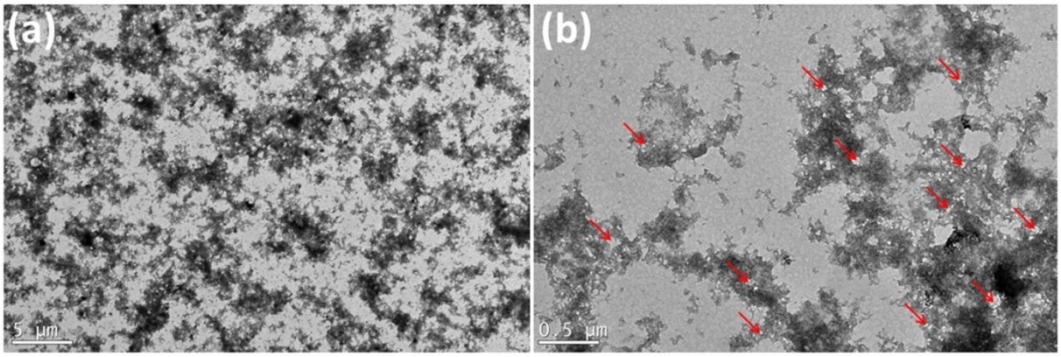

Figure S3. (a-b) The TEM images of Pt/B. The red arrows indicated the defect holes on the Pt/B layers.

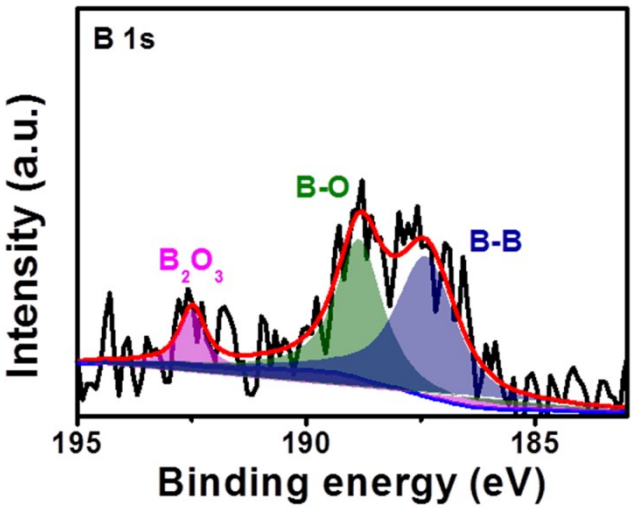

Figure S4. High-resolution B 1s spectrum of Pt/B sample.

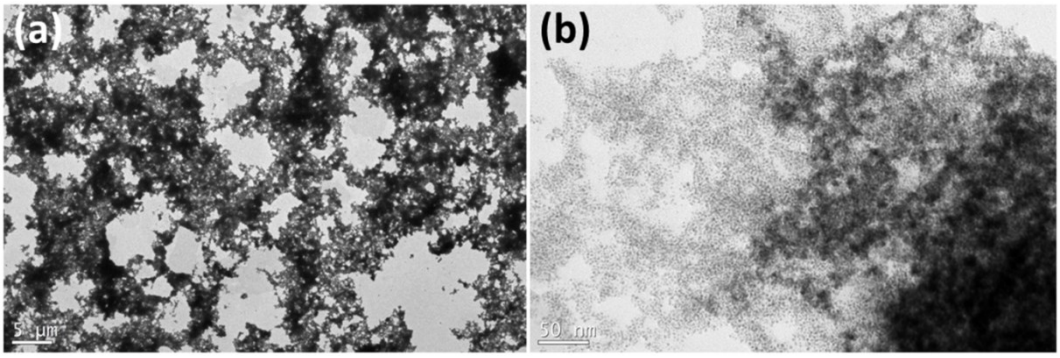

Figure S5. (a-b) The TEM images of stacked Pt/B layer material. Especially, the Pt/B layers stack was obvious between the upper and the under layer in (b).

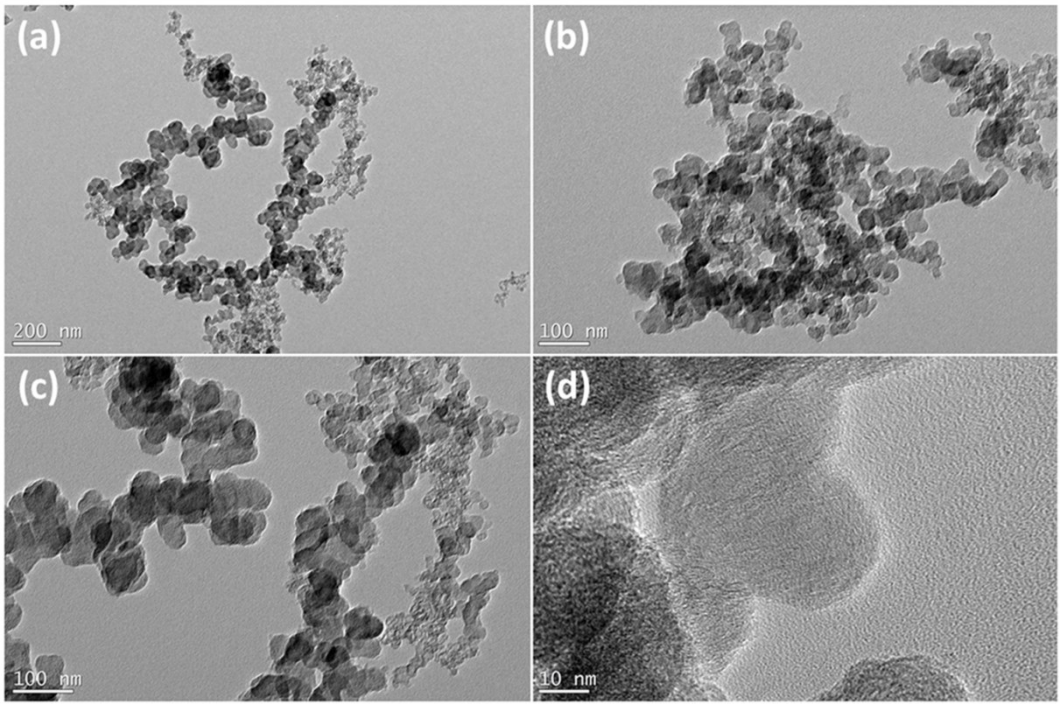

Figure S6. (a-d) TEM images of the raw carbon black without the HB sheets.

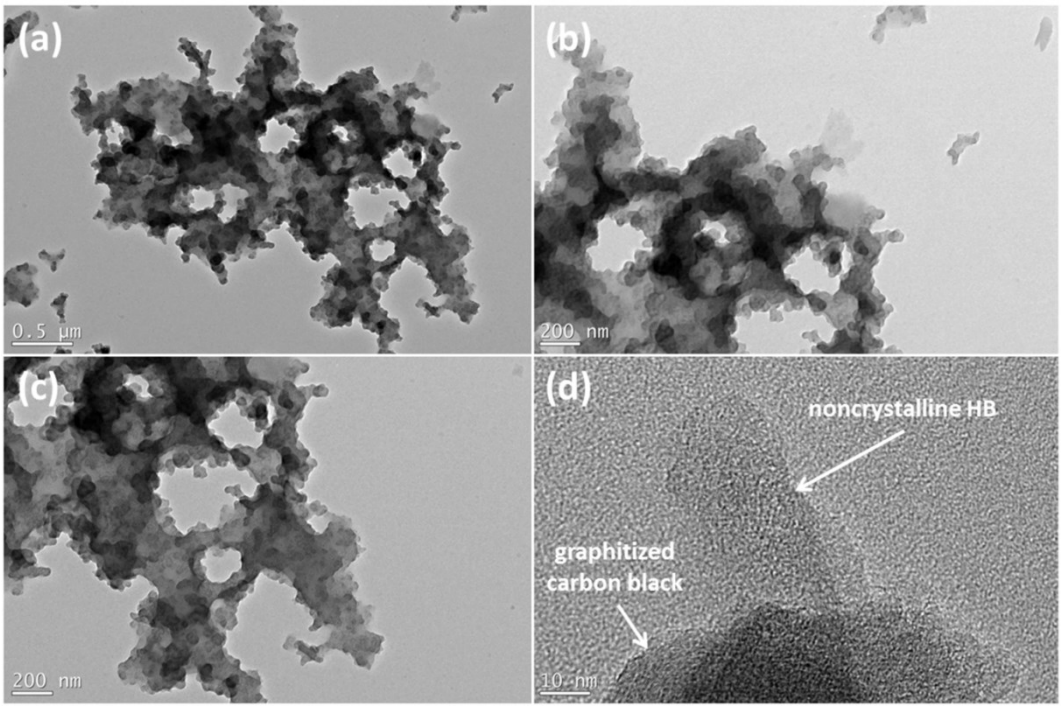

Figure S7. (a-d) TEM images of the HB nanosheets uniformly loaded on carbon black.

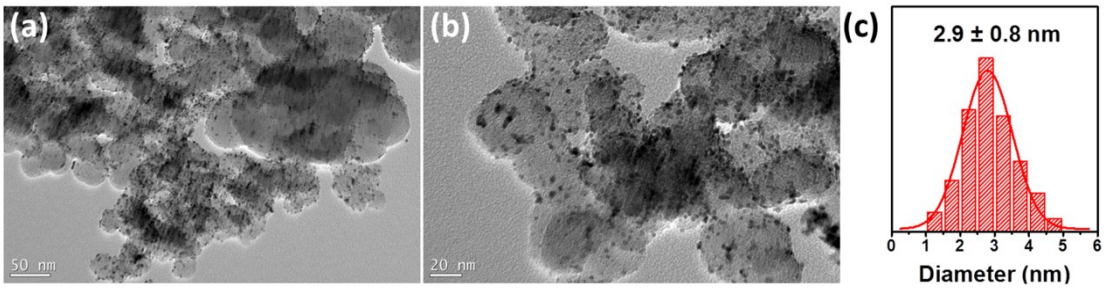

Figure S8. (a-b) The TEM images of the commercial Pt/C. (c) The average diameter and standard deviation of Pt NPs.

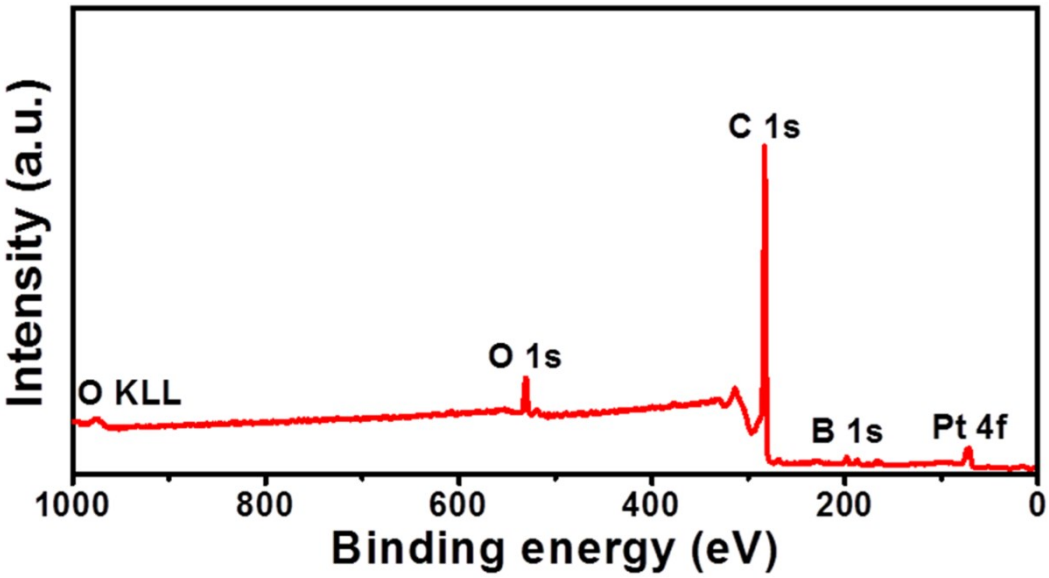

Figure S9. The XPS survey of Pt/B-C (21.2 wt.%).

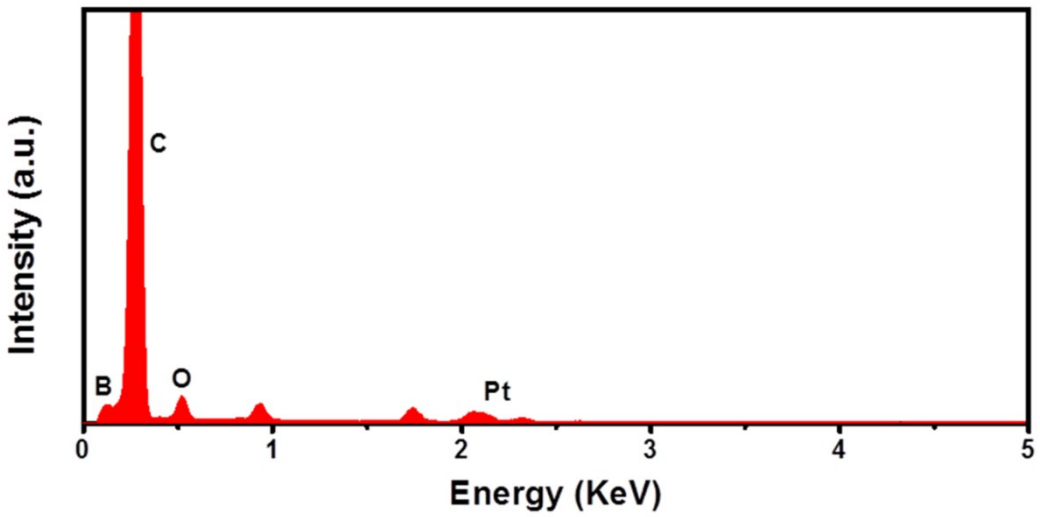

Figure S10. The EDX spectrum of Pt/B-C (21.2 wt.%).

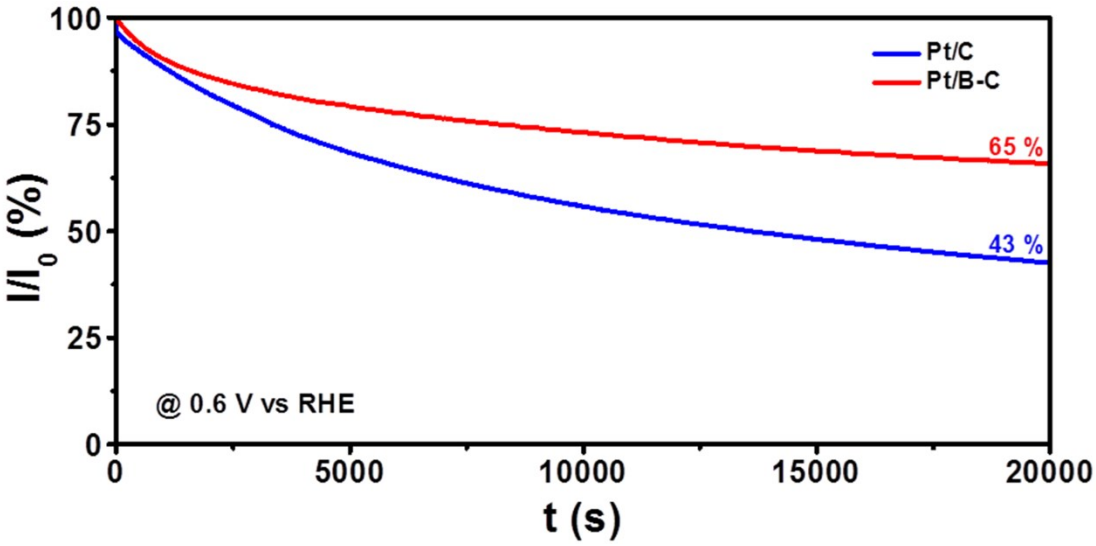

Figure S11. Chronoamperometry tests of commercial Pt/C and Pt/B-C at 0.6 V vs RHE in O_2-saturated 0.1 M $HClO_4$.

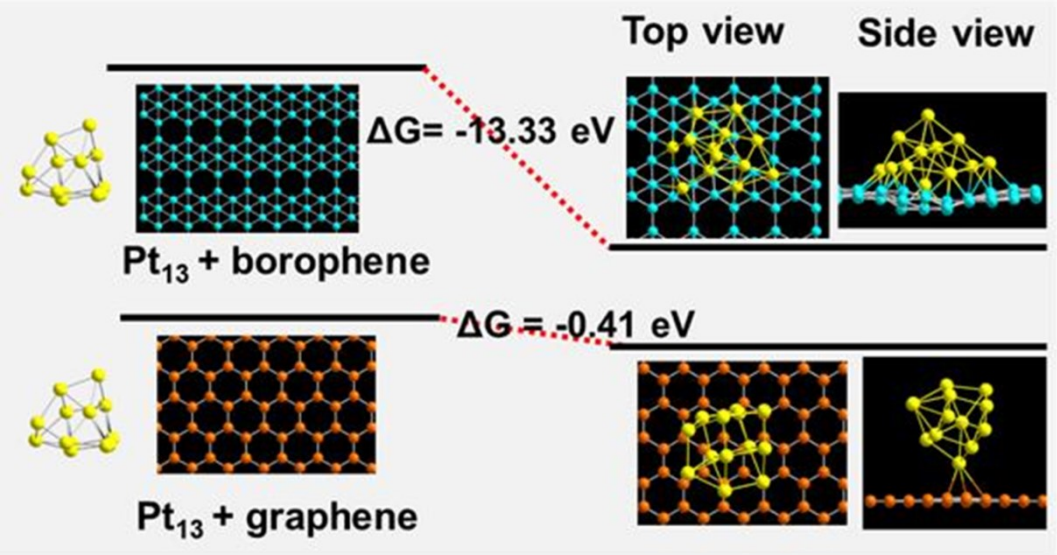

Figure S12. The changes in Gibbs free energy (ΔG) respectively for the systems of Pt_{13} + borophene → Pt_{13}@borophene and Pt_{13} + graphene → Pt_{13}@graphene.

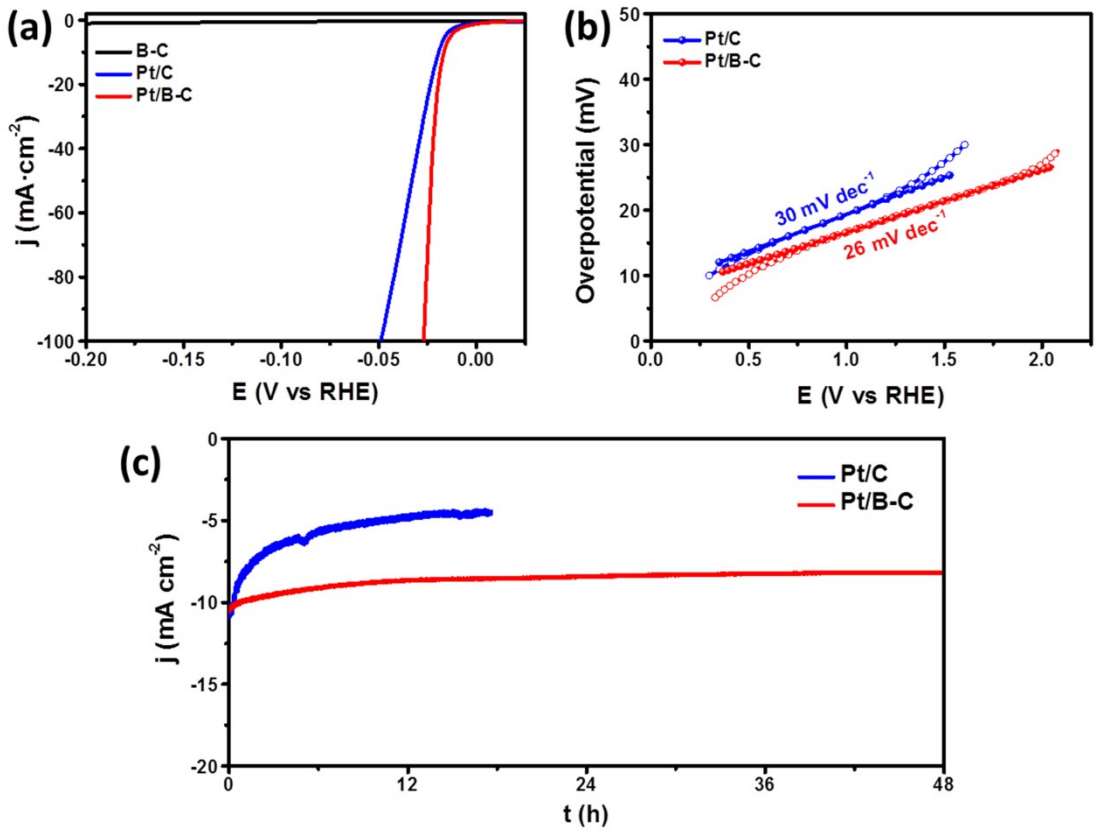

Figure S13. (a) LSVs and (b) Tafel plots of Pt/C and Pt/B-C for HER, respectively. (c) The *i-t* plot of commercial Pt/C and Pt/B-C.

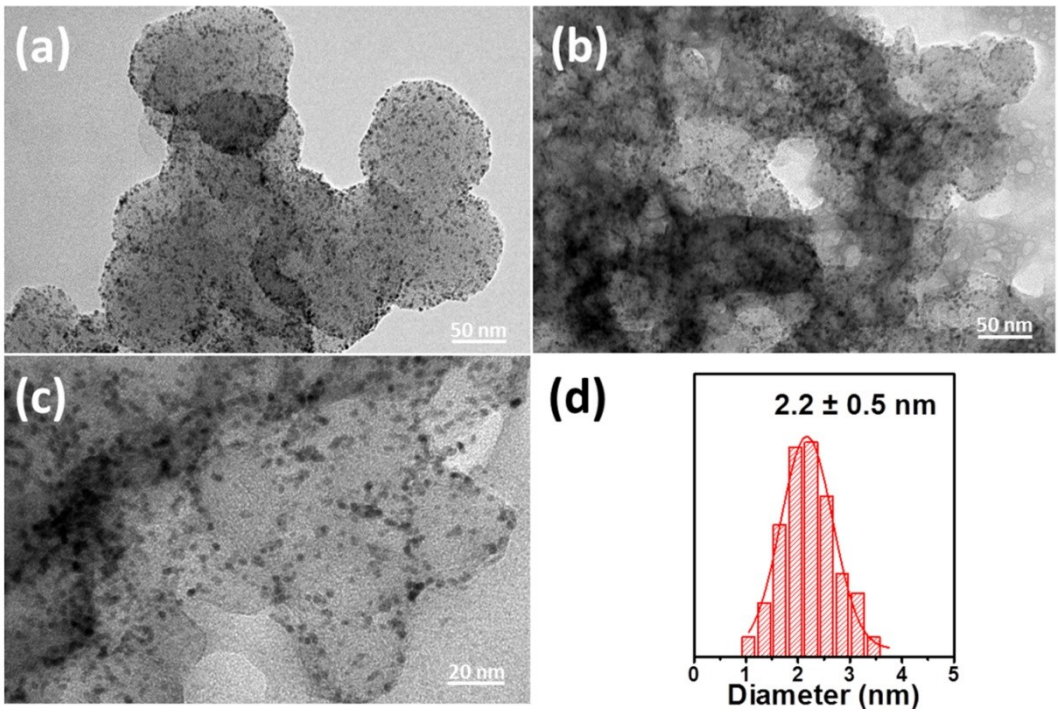

Figure S14. TEM images of (a) original Pt/B-C (21.2 wt.%), and (b-c) after the HER stability test in 0.5 M H_2SO_4 solution. (d) The average diameter and standard deviation of Pt NPs after the HER stability test.

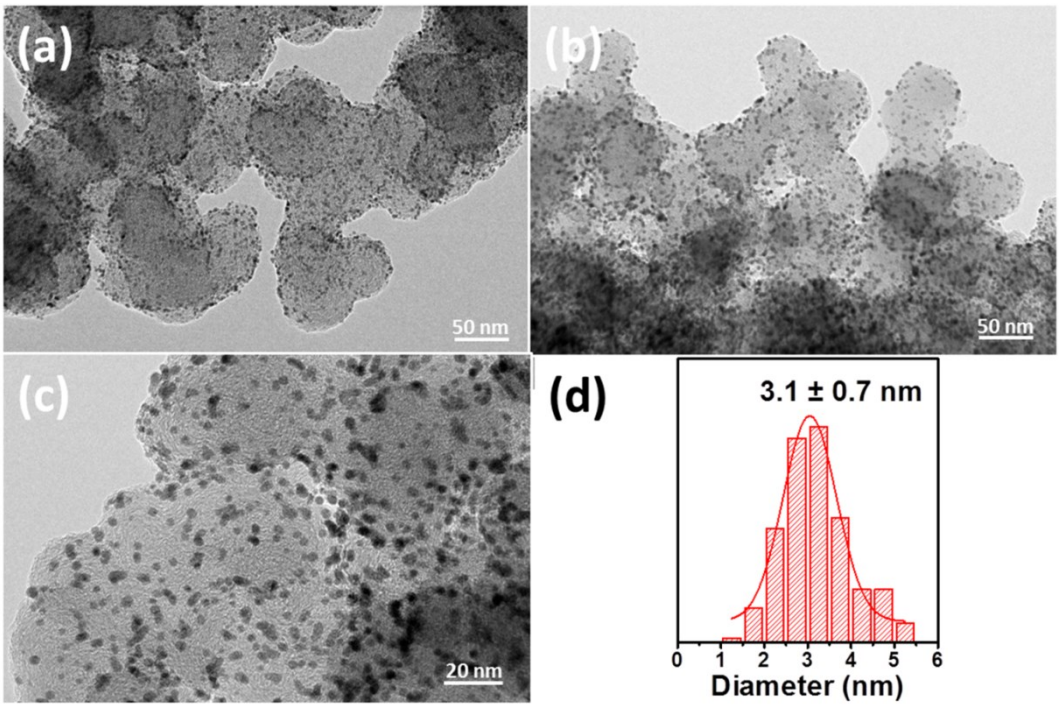

Figure S15. TEM images of (a) original Pt/B-C (21.2 wt.%), and (b-c) after the CA measurement and the long-term durability measurement for MOR. (d) The average diameter and standard deviation of Pt NPs after the CA measurement and the long-term durability measurement.

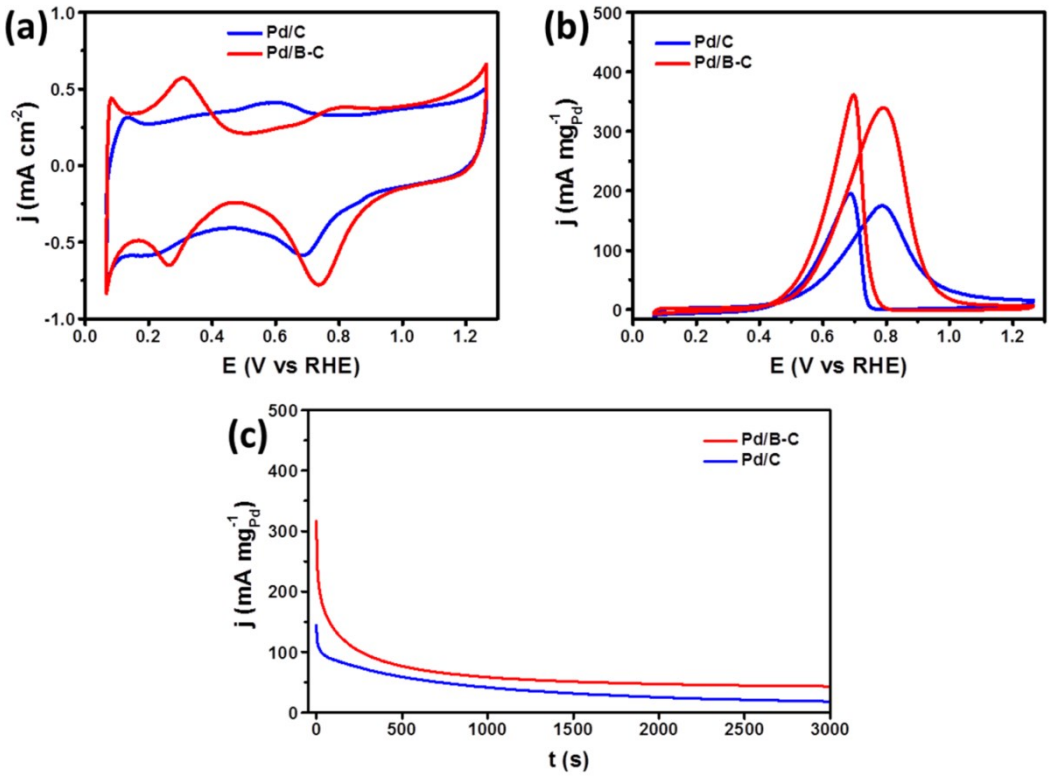

Figure S16. (a) CVs, (b) mass activity curves of commercial Pd/C (10 wt.%) and Pd/B-C (20 wt.%). (c) CA curves at 0.75 V for commercial Pd/C (10 wt.%) and Pd/B-C in N_2-saturated 1 M KOH+0.5 M CH_3CH_2OH with the current normalized by the mass of Pd loading.

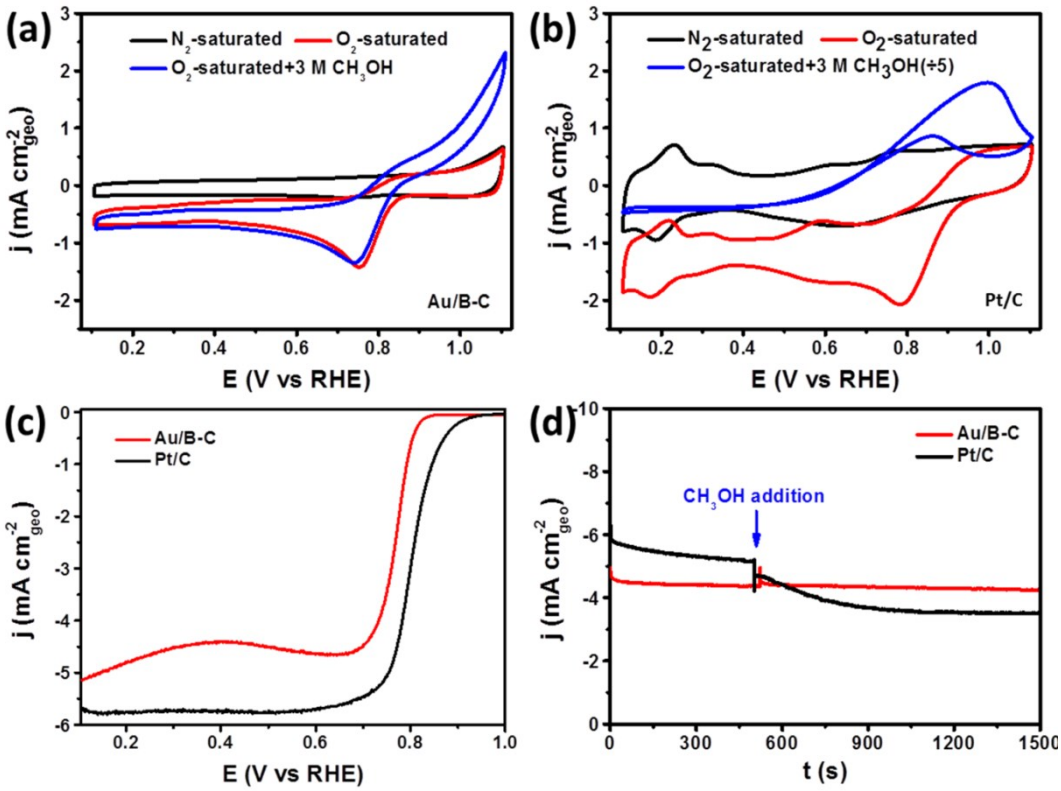

Figure S17. CV curves of (a) Au/B-C (20 wt.%) and (b) commercial Pt/C (20 wt.%). (c) The Polarization curves for ORR of Au/B-C and Pt/C. (d) The *i-t* curves at 0.5 V for the methanol tolerance test of Au/B-C and Pt/C.

For the CV of Au/B-C, a typical ORR peak was observed in O_2-saturated 0.1 M KOH and no significant change of the ORR peak was found in O_2-saturated 0.1 M KOH+3 M CH_3OH. However, as for that of commercial Pt/C, the ORR peak was thoroughly disappeared and the peaks of MOR were predominant. Additionally, the *i-t* curves also showed that the Au/B-C only has a fluctuation, whereas a sharp drop of current density for Pt/C after the addition of methanol.

Table S1. The Pt loading amount in the target products of Pt/B-C (20 wt.%), Pt/B-C (40 wt.%) and Pt/B-C (60 wt.%) were determined from the analysis results of ICP-MS.

	Sample	Pt content (wt%)
1	Pt/B-C (20 wt.%)	21.2
2	Pt/B-C (40 wt.%)	35.4
3	Pt/B-C (60 wt.%)	52.9

References:

[1] H. Nishino, T. Fujita, N. T. Cuong, S. Tominaka, M. Miyauchi, S. Iimura, A. Hirata, N. Umezawa, S. Okada, E. Nishibori, A. Fujino, T. Fujimori, S. Ito, J. Nakamura, H. Hosono, T. Kondo, *J. Am. Chem. Soc.* **2017**, *139*, 13761.

[2] B. Y. Xia, H. B. Wu, X. Wang, X. W. Lou, *J. Am. Chem. Soc.* **2012**, *134*, 13934.

[3] P. E. Blöchl, *Phys. Rev. B* **1994**, *50*, 17953.

[4] G. Kresse, D. P. Joubert, *Phys. Rev. B* **1999**, *59*, 1758.

[5] G. Kresse, J. Furthmülle, *Phys. Rev. B* **1996**, *54*, 11169.

[6] G. Kresse, J. Furthmülle, *Comp. Mater. Sci.* **1996**, *6*, 15.

[7] J. P. Perdew, K. Burke, M. Ernzerhof, *Phy. Rev. Lett.* **1996**, *77*, 3865.

[8] Y. K. Zhang, W. T. Yang, *Phys. Rev. Lett.* **1998**, *80*, 890.

[9] R. P.Feynman, *Phys. Rev.* **1939**, *56*, 340.